Macromolecules

pubs.acs.org/Macromolecules Article

Sustainable Terephthalic Polyesters with Medium/Long Methylene Sequence: Structure−Property Relationships and Closed-Loop Chemical Recycling

Junfeng Liu, Jianfei Xia, Chang Zeng, Chengtao Yu, Ying Zheng, Bao Wang, Shanshan Xu,* and Pengju Pan*

Cite This: *Macromolecules* 2025, 58, 550−561 Read Online

ACCESS | Metrics & More | Article Recommendations | Supporting Information

ABSTRACT: Traditional short-chain terephthalic polyesters such as poly(ethylene terephthalate) (PET) are among the most produced plastics in today's polymer industry, while their large-scale chemical recycling has been a long-standing challenge. The long-chain polyesters have shown good recyclability under mild conditions, whereas the structure−property relationships and chemical recycling performance of long-chain terephthalic polyesters are still unclear. Herein, we synthesized a series of medium/long-chain terephthalic polyesters with different methylene sequence lengths (CH_2 number in diol monomer n_{CH_2} = 6, 8, 10, 12) and investigated their thermal properties, crystallization behavior, mechanical properties, and chemical recycling performance. All terephthalic polyesters show good crystallizability; their melting temperature decreases, and melting enthalpy increases gradually as n_{CH_2} increases from 2 to 12. All polyesters adopt a triclinic crystal lattice while slightly different crystalline lamellar structures. The medium/long-chain terephthalic polyesters exhibit improved ductility and good melt processability, enabling them to be used as three-dimensional (3D) printing materials. In addition, the medium- and long-chain terephthalic polyesters are chemically recyclable and can depolymerize under mild conditions (e.g., 140 °C in methanol). The monomers obtained by depolymerization can be reused to synthesize again the according polyesters. This study provides new inspiration for developing sustainable high-performance polyesters with great industrial potential.

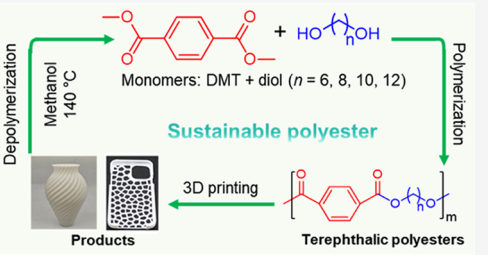

INTRODUCTION

Polyester materials play an indispensable role in today's plastics economy and are widely applied in various fields (e.g., packaging, electronic, automobile, and biomedical fields), due to their excellent physical performances and ease of processability.[1] One of the largest polyester families in the present plastic market is terephthalic polyesters, usually synthesized from the polycondensation of terephthalic acid and diols. Regarding the feedstock of these monomers, terephthalic acid is typically derived from petroleum resources and most aliphatic diols (e.g., 1,3-propanediol, 1,4-butanediol) can be derived from biomass.[2,3] Short-chain terephthalic polyesters such as poly(ethylene terephthalate) (PET) and poly(butylene terephthalate) (PBT) are among the most applied engineering plastics ever developed. Their superior thermal and mechanical properties, high crystallizability, and good barrier properties are particularly interesting for applications in packaging, fiber, textile, etc.[4−6] Compared with PET and PBT, the terephthalic polyesters with longer methylene sequence, denoted as the medium/long-chain terephthalic polyesters, possess enhanced flexibility and toughness, while at the expense of mechanical strength and modulus.[7,8] Meanwhile, the melting point (T_m) of long-chain terephthalic polyesters is also reduced, making melt processing and postrecycling much easier.[9] Obviously, changing the methylene sequence length of the aliphatic diol can be an effective way to regulate the physical properties of terephthalic polyesters.

Despite the extensive pioneer work on short-chain terephthalic polyesters, there has been little research rising for the medium- and long-chain terephthalic polyesters with the methylene number of aliphatic diol (n_{CH_2}) ≥ 6. Some previous reports have elaborated on the crystalline structure, fundamental properties, and deformation behavior of poly(hexamethylene terephthalate) (PHT, n_{CH_2} = 6).[10−12] Compared with the short-chain PET or PBT, PHT exhibits a lower T_g, T_m, and improved ductility. In addition, PHT can be chemically recycled in mild conditions, showing great potential

Received: July 28, 2024
Revised: November 8, 2024
Accepted: December 17, 2024
Published: December 23, 2024

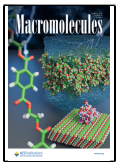

https://doi.org/10.1021/acs.macromol.4c01793
Macromolecules 2025, 58, 550−561

Scheme 1. Synthesis Route of Terephthalic Polyesters

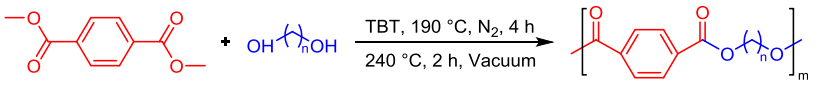

as sustainable plastics.[13,14] However, little attention has been paid to the polyesters in the same family with a longer methylene sequence. Thanks to the development of long-chain diacids and diols from biomass such as plant oil (e.g., castor oil),[15,16] the long-chain polyesters and polycarbonates have thrived over the past decade.[8,17−24] Having a long aliphatic segment separated by the low density of in-chain functional groups (e.g., ester, carbonate, ether), the structure of these polymers can well mimic that of commercial polyethylene (PE),[25,26] with comparable molecular weight, ductility, crystallization rate, and melt processing ability, whereas the thermal property, modulus, and strength are still sacrificed.[27] For that issue, developing PE-like long-chain terephthalic polyesters may be a solution since the presence of benzene rings could serve to maintain relatively high thermal and mechanical properties. Moreover, with sufficiently long methylene segments, the disturbance of benzene-ester parts to the chain conformation of methylene segments would be less significant and therefore may not compromise the crystallizability or macroscopic performance.

Besides the physical properties, the recyclability of polyesters at the end of service life is another important aspect that decides their competitivity as high-performance green plastics in a closed-loop circular economy.[28] Owing to the large presence of ester bonds serving as breaking points, the polyester materials can be chemically recycled into building block monomers while retaining their physical performance.[29] For short-chain terephthalic polyesters such as PET, various solvolysis processes have been proposed, including hydrolysis (in neutral, acidic, or alkaline media), alcoholysis, glycolysis, aminolysis, and enzymatic hydrolysis, while only a few of which has been established on an industrial scale.[1,30−34] The major problem hindering the successful implementation in industry lies in the exigent conditions required for depolymerization (e.g., high temperature range of 200−300 °C, high pressure),[35] making the recycling route much less cost-effective. Interestingly, for the medium/long-chain polyesters, their relatively low T_m could allow them to be chemically recycled in milder conditions. Usually, the solvolysis can be conducted in the 120−150 °C range at high efficiency, and a complete deconstruction into monomers can be achieved under these mild conditions.[24,36−40] For instance, Mecking and co-workers have reported to depolymerize the long-chain polyesters prepared from 1,18-octadecane diol and 1,18-dimethyl octadecanedioate at 120 °C in methanol in 24 h with a recycling rate >96%.[24] Based on these former studies on the long-chain aliphatic polyesters, it can be imagined that medium/long-chain terephthalic polyesters should also be easily chemically recovered under mild conditions, considering the flexibility of aliphatic chain segments, low density of rigid terephthalic acid units, and the presence of ester bonds as break points. However, up to now, a fine report on the structure−property relationships of medium/long-chain terephthalic polyesters and their detailed recovery process, depolymerization kinetics, and performance of recovered products is still lacking, despite its great significance in guiding the processing and practical applications of terephthalic polyesters.

To elaborate on the structure−property relationships and chemical recycling behavior of terephthalic polyesters, we synthesized a series of medium/long-chain polyesters with different methylene sequence lengths (n_{CH_2} = 6, 8, 10, 12). The short-chain PET and PBT were also studied for comparison. A comprehensive relationship between chemical structure and thermal properties, crystalline structure, mechanical properties, and chemical recycling performance was established. The medium/long-chain terephthalic polyesters show good crystallizability and melt processability with the T_m decreasing gradually as n_{CH_2} increases. Moreover, the synthesized polyesters are able to depolymerize under mild conditions (∼140 °C) and the obtained monomers can be reused to synthesize again the according polyesters with similar properties to those of virgin ones. This study provides new inspiration for developing sustainable polyesters with great industrial potential.

RESULTS AND DISCUSSION

Synthesis and Characterization of Medium/Long-Chain Terephthalic Polyesters. The medium/long-chain terephthalic polyesters with various methylene sequence lengths were prepared through melt polymerization using dimethyl terephthalate (DMT) and different diols as monomers (Scheme 1). The synthesized polyesters include poly(hexamethylene terephthalate) (PHT, n_{CH_2} = 6), poly(octamethylene terephthalate) (POT, n_{CH_2} = 8), poly(decamethylene terephthalate) (PDT, n_{CH_2} = 10), and poly(dodecylmethylene terephthalate) (PDeT, n_{CH_2} = 12). The chemical structures of synthesized polyesters were characterized by ^{1}H NMR. As shown in Figure 1, the peaks observed at 8.00 ppm (a) are attributed to protons on the benzene rings. The peaks observed at 4.27 (b), 1.74 (c), and

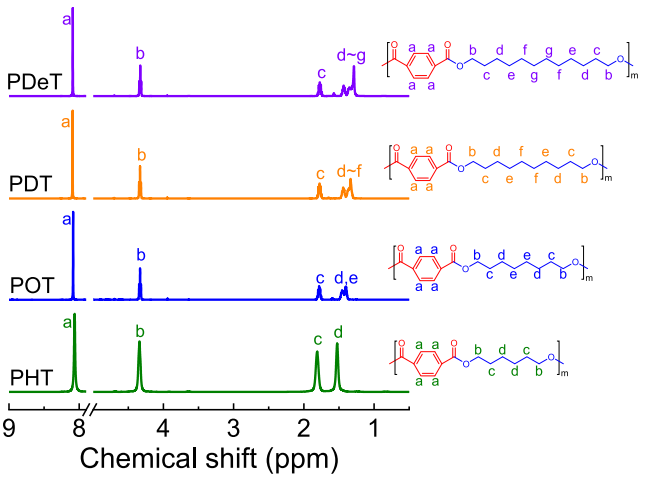

Figure 1. ^{1}H NMR spectra of PHT, POT, PDT, and PDeT.

https://doi.org/10.1021/acs.macromol.4c01793
Macromolecules 2025, 58, 550−561

1.46 ppm (d) are attributed to the CH_2 protons at different positions of the aliphatic carbon chain. As n_{CH_2} increases from 6 to 12, some overlapping peaks attributed to CH_2 protons appear at 1.45−1.20 ppm (e, f, g).

The molecular characteristics of synthesized polyesters were summarized in Table 1. As seen in Table 1, the absolute weight-average molecular weights (M_w) of PHT, POT, PDT, and PDeT range from 47.3 to 56.3 kg/mol, with a polydispersity index (PDI) of ∼1.5. Since PET and PBT with short methylene sequence lengths are insoluble in the common solvents such as chloroform, their M_w and PDI were not determined by gel permeation chromatography (GPC). The intrinsic viscosity, [η], of all polyesters are within 0.96−1.1 dL/g, similar to the values of commercialized PET (0.95 dL/g) and PBT (0.89 dL/g), indicating the relatively high molecular weight of synthesized polyesters. These characterization results confirm the successful synthesis of medium- and long-chain polyesters with high molecular weights.

Table 1. Molecular Characteristics of Terephthalic Polyesters

sample	n_{CH_2} [a]	M_n [b] (kg/mol)	M_w [b] (kg/mol)	PDI [b]	[η] [c] (dL/g)
PHT	6	37.7	55.1	1.46	0.96
POT	8	30.8	47.3	1.54	1.02
PDT	10	37.0	56.3	1.52	1.10
PDeT	12	32.4	49.8	1.54	1.07

[a]CH_2 number in the diol monomer. [b]Absolute weight and number-averaged molecular weights (M_w, M_n) as well as PDI measured by GPC coupled with light scattering detector. [c]Intrinsic viscosity.

Crystallization and Melting Behavior. The crystallization and melting behavior of all terephthalic polyesters were first investigated by differential scanning calorimetry (DSC). Figure 2a,b shows the DSC curves collected during cooling from the melt and subsequent heating process. All polyesters exhibit a single crystallization peak during the cooling process. The crystallization peak of PET was relatively broad while other polyester samples had sharper crystallization peaks, indicating the lower crystallization rate of PET compared with other polyesters with longer methylene sequences. All polyesters have a major melting peak during the subsequent heating process.

The characteristic temperatures and enthalpies related to the crystallization and melting processes of polyesters are evaluated from the DSC curves, and their evolutions with an increase of n_{CH_2} are depicted in Figure 2c,d. With n_{CH_2} increasing from 2 to 12, the crystallization temperatures (T_c) of polyesters decrease monotonically from 186.3 to 86.5 °C, while the associated crystallization enthalpy (ΔH_c) decreases from −49.5 to −56.9 J/g. The melting temperature (T_m) of polyesters also decreases monotonically from 251.3 to 121.7 °C, while the melting enthalpy (ΔH_m) increases from 41.2 to 51.8 J/g as n_{CH_2} increases from 2 to 12. Such decreases in T_c and T_m values with n_{CH_2} could originate from a reduced density of rigid terephthalic acid units with the increase of flexible methylene segments. The increased chain flexibility leads to a higher conformational entropy (ΔS), thus effectively lowering the T_m ($T_m \sim \Delta H/\Delta S$).[41] Meanwhile, it would be easier for longer methylene segments to orderly arrange and crystallize,[42] therefore resulting in the observed increase of ΔH_c and ΔH_m

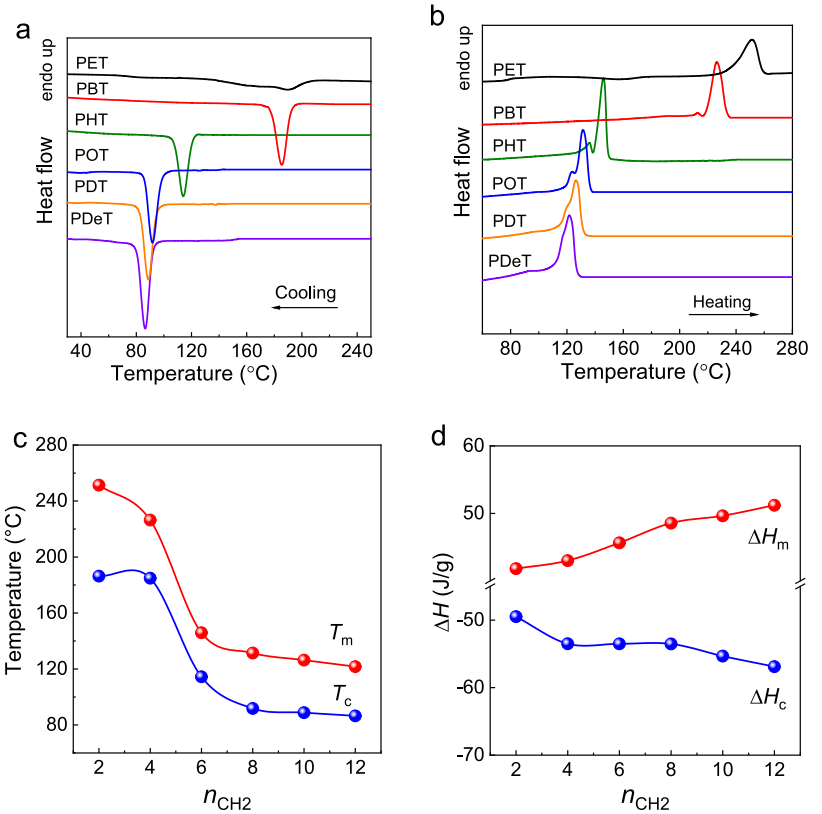

Figure 2. DSC results of terephthalic polyesters with various methylene sequence lengths. (a) DSC curves collected during cooling from the melt state; (b) DSC curves collected during subsequent heating scans; (c, d) changes of (c) T_c, T_m and (d) ΔH_c, ΔH_m with methylene sequence length.

https://doi.org/10.1021/acs.macromol.4c01793
Macromolecules 2025, 58, 550−561

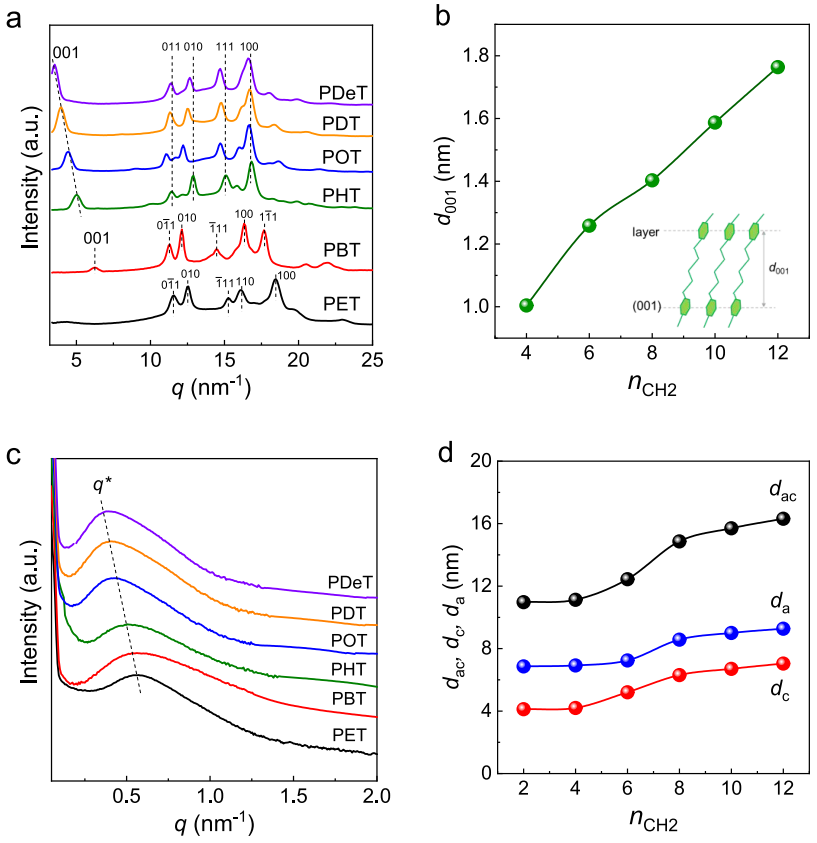

Figure 3. Crystalline structures of terephthalic polyesters after melt crystallization at T_c = 100 °C: (a) WAXS profiles; (b) evolution of *d*-spacing of (001) plane d_{001} with n_{CH_2}. Inset: a schematic presentation of layer structure formed by phenylene groups; (c) SAXS profiles; (d) evolutions of d_{ac}, d_c, and d_a with n_{CH_2}.

values. The increase in chain flexibility with a longer methylene sequence is also confirmed by the evolution of T_g values with greater n_{CH_2} (Figure S1). The T_g values of PET, PBT, PHT, POT, PDT, and PDeT (n_{CH_2} increasing from 2 to 12) were determined to be 71.9, 44.1, 17.4, 10.2, 2.1, and −2.2 °C, respectively, well indicating a gradually improved chain mobility in long-chain polyesters.

We note that compared with the short-chain polyesters PET and PBT, the T_c and T_m of polyesters reduce greatly by ∼70 °C when n_{CH_2} increases from 4 to 6. However, similar T_c (86.5−91.8 °C) and T_m (121.7−131.7 °C) are detected for the long-chain polyesters with $n_{CH_2} \geq 8$ (e.g., POT, PDT, and PDeT). This indicates that the crystalline structure and molecular chain arrangements between short- and long-chain terephthalic polyesters might be different. We further discuss this point in the next section along with the wide angle X-ray scattering/small angle X-ray scattering (WAXS/SAXS) results. In addition, the ΔH_c and ΔH_m values of the long-chain terephthalic polyesters with $n_{CH_2} \geq 8$ are less dependent on n_{CH_2}, ranging from −53.5 to −56.9 J/g and from 48.7 to 51.2 J/g, respectively. Therefore, it is inferred that when the methylene sequence length grows to a certain extent, the thermal properties of terephthalic polyesters tend to be little affected by n_{CH_2}.

Crystalline Structure. The effect of the methylene sequence length on the crystalline structure of terephthalic polyesters was investigated by WAXS and SAXS. All samples for WAXS and SAXS analyses were treated by isothermal melt crystallization at T_c = 100 °C after melting at 270 or 180 °C for 5 min. Sharp and defined diffraction peaks are observed in the WAXS curves of all polyester samples (Figure 3a), indicating that the polyesters are well crystallized with a relatively high crystallinity. For PET, the characteristic diffraction peaks detected at q = 11.6, 12.6, 15.3, 16.1, and 18.5 nm^{-1} from $(0\bar{1}1)$, (010), $(\bar{1}11)$, (110), and (100) planes are assigned to the crystals with triclinic unit cell (a = 0.46 nm; b = 0.59 nm; c = 1.08 nm; α = 98°; β = 118°; γ = 112°).[43] For PBT, the characteristic peaks detected at q = 6.2, 11.3, 12.1, 14.4, 16.3, and 17.7 nm^{-1} from (001), $(0\bar{1}1)$, (010), $(\bar{1}11)$, (100), and $(1\bar{1}1)$ planes are assigned to the α crystal phase with triclinic unit cell (a = 0.48 nm; b = 0.59 nm; c = 1.16 nm; α = 99°; β = 115°; γ = 111°).[44] For PHT, the characteristic peaks are detected at q = 5.1, 11.5, 12.9, 15.1, and 16.9 nm^{-1} from (001), (011), (010), (111), and (100) planes, assigning to the triclinic β crystal phase formed at T_c = 100 °C with unit cell a = 0.48 nm, b = 0.57 nm, c = 1.57 nm, α = 104°, β = 116°, and γ = 108°.[10] The long-chain terephthalic polyesters with $n_{CH_2} \geq 8$ also produce the triclinic crystals at T_c = 100 °C, showing a similar WAXS pattern as PHT except for the slight difference in peak position.[18] The similarity of diffraction patterns among these long-chain polyesters suggests that they have similar chain conformations and interchain packing in the crystal unit cell.

However, compared with the short-chain polyesters PET and PBT, the peak shape and position of WAXS patterns are clearly different for the long-chain polyesters, which again

https://doi.org/10.1021/acs.macromol.4c01793
Macromolecules 2025, 58, 550−561

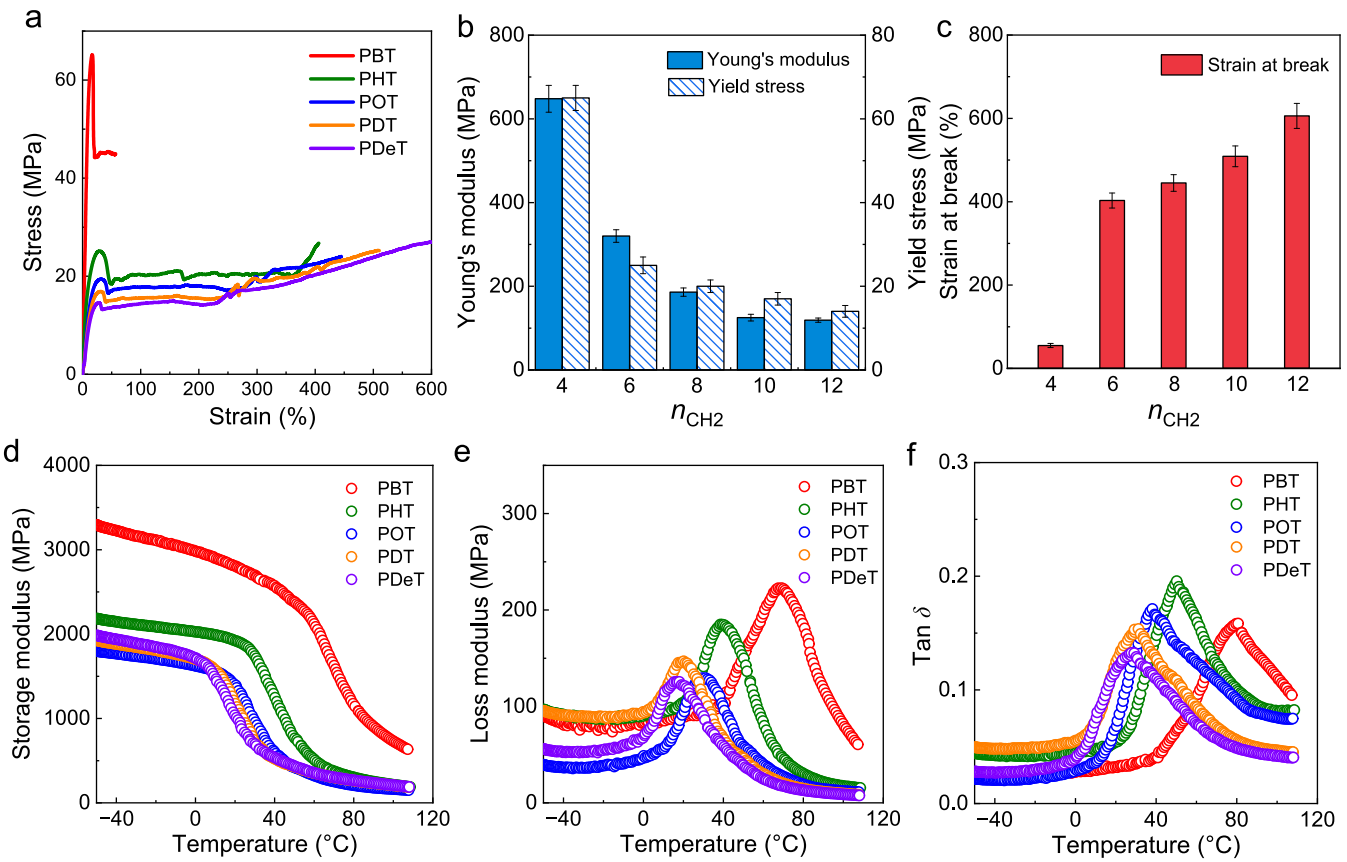

Figure 4. Mechanical and thermomechanical properties of terephthalic polyesters. (a) Stress−strain curves; (b, c) changes of (b) Young's modulus, yield stress, and (c) strain at break with n_{CH_2}. (d−f) Temperature-variable evolutions of (d) the storage modulus, (e) the loss modulus, and (f) tan δ. All samples were treated by melt crystallization at T_c = 100 °C for 1 h before the measurements.

suggests the difference in crystal structure between the short- and long-chain polyesters. For instance, we noticed that the peak position of the (001) plane varies with the methylene sequence length n_{CH_2}. For PET, the close chain packing between crystalline molecules would force the phenylene groups to slip past each other, therefore no obvious diffraction from the (001) plane reflecting the long-range order of layer structure is observed.[45] For the medium- and long-chain polyesters, diffraction from the (001) plane is well detected, indicating the formation of layer structure by phenylene groups (Figure 3b, inset).[46] The peak intensity of the (001) plane steadily intensifies with greater n_{CH_2}, which is a sign of perfection of the formed layer structure, due to the improved chain mobility with longer flexible methylene segments. Meanwhile, the peak position continuously shifts to the low-q region, indicating an increase of d-spacing ($d = 2\pi/q$) from 1.01 to 1.76 nm when n_{CH_2} increases from 4 to 12. Such an increase of d_{001} should be attributed to the longer repeat unit length in the crystal unit cell of long-chain polyesters.[47]

We have also calculated the theoretical repeat unit length l of these polyesters with all-*trans* planar chain conformation using $l = 0.125n + 0.822$, with 0.125 and 0.822 nm being the length of one *trans* CH_2−CH_2 bond and one terephthalate ester part along chain axis.[46] As a result, l increases from 1.32 to 2.32 nm when n_{CH_2} increases from 4 to 12, which are all larger than the obtained d_{001} values. The differences between l and d_{001} suggest that the molecular chains in these terephthalic polyesters are inclined with respect to the normal of the phenylene group layer and probably adopt some contract conformation (e.g., *gauche* bonds). Combined with DSC results (Figure 2), we conclude that the effect of methylene sequence length on the crystal structure and thermal properties of terephthalic polyesters is most significantly observed in the short-to-medium length range (n_{CH_2} = 2−6), while such an effect is much less obvious when n_{CH_2} exceeds a critical value ($n_{CH_2} \geq 8$).

Crystalline lamellar structures of terephthalic polyesters were also characterized by SAXS. As illustrated in Figure 3c, all samples show a single broad scattering peak, and the peak position (q^*) shifts steadily to the low-q region when n_{CH_2} increases. Accordingly, the long period (d_{ac}) can be calculated by Bragg's equation ($d_{ac} = 2\pi/q^*$). The thickness of crystal lamellae (d_c) and that of the amorphous layer (d_a) were estimated by a 1D electron density correlation function (Figures S2 and S3). Figure 3d depicts the evolutions of d_{ac}, d_c, and d_a as a function of n_{CH_2}. The d_{ac}, d_c, and d_a all increase monotonically as n_{CH_2} increases. This suggests that the longer the CH_2 sequence is, the thicker the crystal lamellae and amorphous layer are. We note that d_{ac}, d_c, and d_a all increase significantly when n_{CH_2} increases from 4 to 6. This further demonstrates the difference in crystalline structure between short- and long-chain terephthalic polyesters, especially in the short-to-medium chain length range (n_{CH_2} = 2−6).

Mechanical and Thermomechanical Properties. To further elucidate the relationship between microstructure and

https://doi.org/10.1021/acs.macromol.4c01793
Macromolecules 2025, 58, 550−561

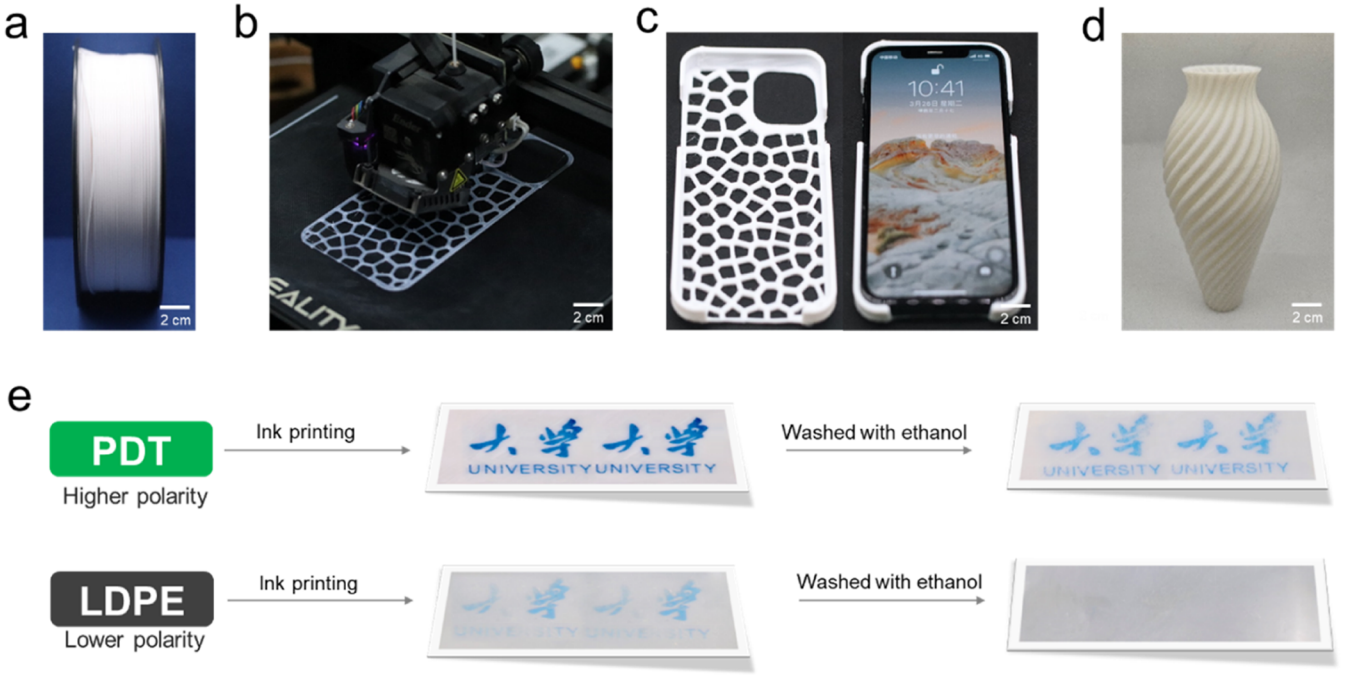

Figure 5. 3D printing and dyeability of terephthalic polyesters (using PDT as an example). (a–d) Photos illustrating the (a) melt-extruded filaments, (b) 3D printing process, (c) printed phone cover, and (d) vase. (e) Schematic illustrations of ink printing and washing on LDPE and PDT surfaces.

macroscopic properties of terephthalic polyesters, uniaxial tensile tests were performed on the polyester specimens obtained by melt crystallization at T_c = 100 °C. The stress–strain curves of all polyesters are shown in Figure 4a. It can be seen from Figure 4a that all polyesters undergo plastic deformation after yield, while their plastic deformation behaviors are different. The short-chain polyester (e.g., PBT) shows a distinct strain softening and fails quickly after yielding, whereas the medium/long-chain polyesters all exhibit stable plastic deformation toward strain hardening at large strain. The yield stress, Young's modulus, and strain at break were evaluated from the stress–strain curves and are depicted in Figure 4b,c. It can be seen that the medium/long-chain polyesters (n_{CH_2} = 6–12) are indeed more flexible than the short ones. The yield stress and Young's modulus continue to decrease with n_{CH_2} increasing from 4 to 12, with the former decreasing from 65 to 14 MPa and the latter decreasing from 648 to 120 MPa. On the contrary to the evolutions of yield stress and Young's modulus, the strain at break increases from 55 to 605%, showing an enhanced ductility with the increase of methylene sequence length. Therefore, control over the methylene sequence length could be an effective way to regulate the mechanical properties of terephthalic polyesters.

Besides the uniaxial mechanical properties, the dynamic mechanical properties of polymeric materials are also of great importance to estimate their macroscopic performances in practical applications. Therefore, we also investigated the thermomechanical properties of terephthalic polyesters by DMA and the temperature-dependent evolutions of storage modulus, loss modulus, and loss tangent (tan δ) are shown in Figure 4d–f. In the glassy plateau region, the storage modulus of polyesters systematically decreases from ~3300 to ~1800 MPa with n_{CH_2} increasing from 4 to 12. Such a decrease of storage modulus is in line with the evolution tendency of elastic modulus discussed previously (Figure 4b), which manifests a reduced stiffness of long-chain terephthalic polyesters.[48] All samples show a sudden drop of storage modulus upon heating in the 8–70 °C region, known as the α relaxation. The precise α relaxation temperature, determined from the peak position of the loss modulus (Figure 4e), decreases steadily from ~68 to ~12 °C when n_{CH_2} increases from 4 to 12, which suggests a higher chain mobility in the long-chain polyesters. Their low α relaxation temperature can ensure a good flexibility of amorphous chains at room temperature, thus allowing the large plastic deformation observed on the tensile test (Figure 4a).[49]

The evolutions of loss modulus and tan δ can give more information about the molecular dynamics of terephthalic polyesters. Figure 4e shows that the peak of loss modulus shifts continuously to the low-temperature region, and the magnitude of the peak decreases when n_{CH_2} increases. The decrease of peak temperature and magnitude in the loss modulus curve may reflect a reduction of rigid segmental fraction inside the polyester.[50] Likely, the peak temperature of tan δ also shows a similar decrease trend with n_{CH_2} increasing. Since the tan δ peak is related to the cooperative motion from repeat units of different chains,[51] it can be inferred that the terephthalic polyester gradually evolves from a rigid material with restricted molecular motions into a flexible one with largely enhanced chain mobility with n_{CH_2} increasing.

Processability Evaluated by Three-Dimensional (3D) Printing. Previous results have demonstrated that the long-chain terephthalic polyesters have relatively low T_m, fast crystallization rate, and good flexibility, making them particularly suitable for melt processing.[52] To explore their processabilities for additive manufacturing, we took PDT as an example and evaluated its 3D printing behavior. Figure 5a–d shows the 3D printing process and the resulting products. The

https://doi.org/10.1021/acs.macromol.4c01793
Macromolecules 2025, 58, 550–561

Scheme 2. Depolymerization Reaction Scheme of Medium/Long-Chain Terephthalic Polyesters

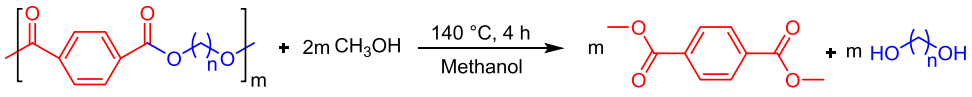

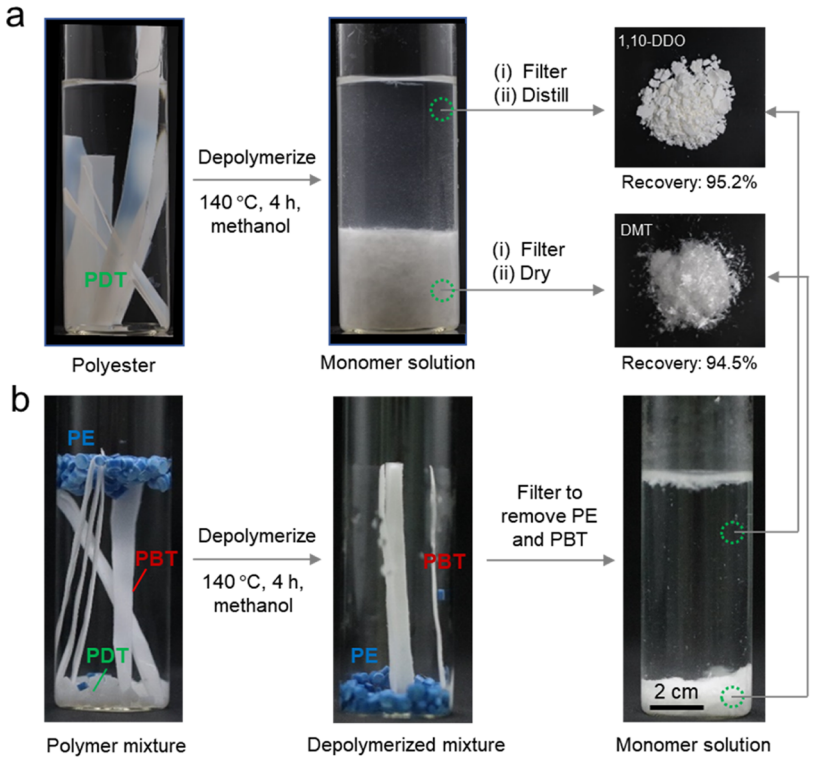

Figure 6. Illustration of chemical recycling process: (a) PDT and (b) PDT with the presence of LDPE and PBT. All photos were taken at 25 °C.

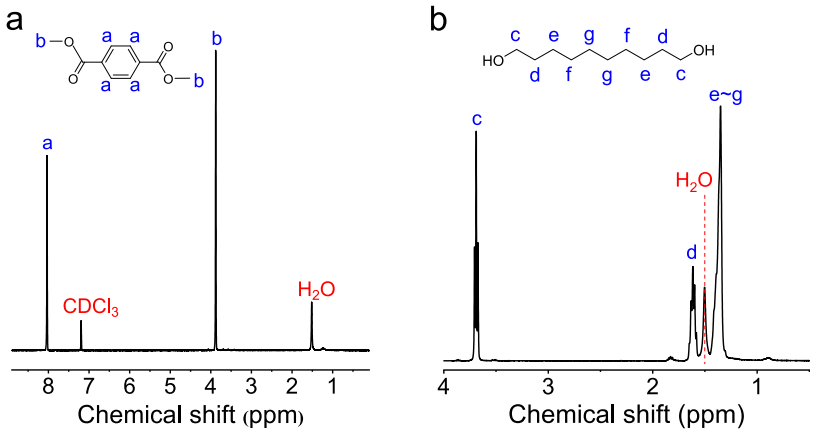

Figure 7. ^{1}H NMR spectra of depolymerized products for PDT: (a) recycled DMT and (b) recycled 1,10-DDO.

layer-bed temperature of 3D printing was set at 50 °C, at which temperature PDT can crystallize quickly within seconds. The elastic modulus of PDT is around 150 MPa, which can withstand a certain weight without deformation. Therefore, handicrafts such as mobile phone shells and vases could be prepared by 3D printing, as demonstrated in Figure 5c,d.

Compared with traditional 3D printing materials such as low-density polyethylene (LDPE), long-chain terephthalic polyesters have higher polarity due to the presence of many ester bonds, enabling direct printing of ink on the material surface (Figure 5e). The ink printed on the polyester surface could be retained even when cleaned by a polar solvent such as ethanol, demonstrating the good dyeability of the long-chain terephthalic polyesters. On the contrary, the ink cannot be well printed on the surface of LDPE and it can also be completely washed by a polar solvent such as ethanol. Therefore, long-chain terephthalic polyesters show great potential as a new type of 3D printing polymer material with good dyeability.

Depolymerization and Chemical Recycling. Finally, the chemical recyclability of terephthalic polyesters was investigated to evaluate their potential toward sustainable materials. The depolymerization of polyesters was conducted at 140 °C in methanol (1.0 g of polymer in 25 mL of methanol),[53] as illustrated in Scheme 2. The chemical recycling routes of PDT

https://doi.org/10.1021/acs.macromol.4c01793
Macromolecules 2025, 58, 550−561

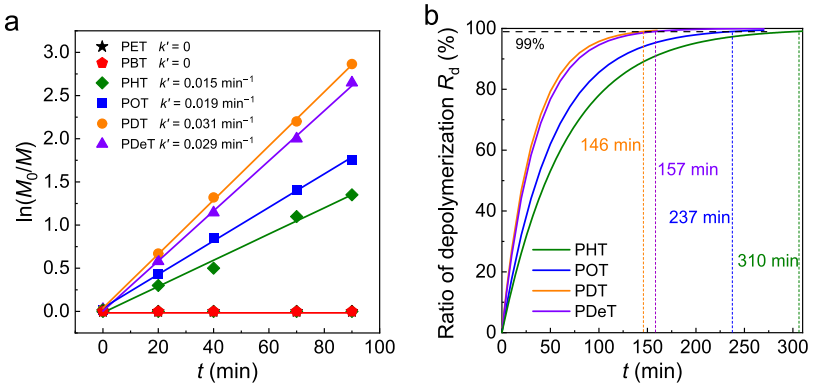

Figure 8. Depolymerization kinetics of terephthalic polyesters: (a) evolution of $\ln(M_0/M)$ with t expressed by measured data points and their fitting curves. (b) Theoretical change of depolymerized ratio R_d with reaction time calculated from eq 4.

in the neat state and in a polymer mixture (containing PE, PBT, and PDT) are illustrated in Figure 6. As seen in Figure 6a, the long strips of PDT had decomposed into small white particles after 4 h of the depolymerization reaction. During cooling down to room temperature (central pictures), the precipitation of DMT began to take place, and the obtained mixture solution was then held at 0 °C for 1 h to completely precipitate in terms of needle-like white solid, with a recovery rate of 94.5%. The filtrate was then subjected to rotary evaporation to remove methanol and the remaining bulk-like white solid was 1,10-DDO, having a recovery rate of 95.2%. Since the polymer blends were commonly used in practical applications, the chemical recycling of PDT was also evaluated with the presence of other polymer strips such as LDPE and PBT, as illustrated in Figure 6b. In the polymer mixture, PDT could still be accurately recovered while the LDPE and PBT strips remained in their original state and did not depolymerize after depolymerization in methanol at 140 °C for 4 h.

Chemical structures of depolymerized products were further characterized by ^{1}H NMR. Figure 7 shows the ^{1}H NMR spectra of recycled products from the depolymerization of PDT. As depicted in Figure 7a, the ^{1}H NMR spectrum of the obtained needle-like white solid (Figure 6a) shows resonance peaks attributed to the protons on the benzene ring and to the $-OCH_3$ protons at 8.00 (peak a) and 3.88 ppm (peak b), respectively, proving that the recovered solid is indeed DMT with high purity. For the bulk-like white solid (Figure 6a), its ^{1}H NMR spectrum (Figure 7b) shows the resonance peak attributed to $-OCH_2$ protons at 3.57 ppm (peak c) and multiple peaks attributed to the CH_2 protons at 1.70−1.10 ppm. By calculating the peak area ratio of $-OCH_2$ and CH_2 proton peaks ($A_{OCH_2}/A_{CH_2} = 4$), it can be confirmed that the bulk-like white solid is 1,10-DDO with high purity. In the case of PHT, POT, and PDeT, the ^{1}H NMR spectra of the accordingly depolymerized products also confirmed that DMT, 1,6-HDO, 1,8-ODO, and 1,12-DeDO were successfully obtained after depolymerization (Figure S4).

The depolymerization kinetics of terephthalic polyesters was further investigated. In this experiment, the terephthalic polyesters were first depolymerized at 140 °C at different times. Afterward, the mixed solution was filtered, and the obtained monomers (DMT/diol) were removed from the filter. The remaining filter residue was considered in the nondepolymerized polyesters. Theoretically, the depolymerization reaction rate can be expressed as[54]

$$-\frac{d[P]}{dt} = k[P][CH_3OH]^n \quad (1)$$

where $[P]$ is the concentration of terephthalic polyester at a certain reaction time t, $[CH_3OH]$ is the concentration of methanol, k is the reaction rate constant, and n is the reaction order. Owing to excessive methanol, the depolymerization can be considered as a pseudo-first-order reaction ($n \sim 1$). By integrating eq 1, it can be obtained:

$$\ln\frac{[P]_0}{[P]} = k't \quad (2)$$

where $k' = k[CH_3OH]$, and $[P]_0$ is the initial concentration of terephthalic polyester before depolymerization. Owing to the absence of gas-phase products and the presence of excess methanol, $[P]_0/[P]$ equals to M_0/M, therefore eq 2 becomes

$$\ln\frac{M_0}{M} = k't \quad (3)$$

where M_0 and M are the mass of terephthalic polyester before depolymerization reaction and at time t, respectively. Therefore, the reaction rate constant k' can be determined from the slope of the $\ln(M_0/M)$ vs t curve. The theoretical depolymerization ratio R_d can then be calculated as

$$R_d = 1 - \frac{M}{M_0} = 1 - \frac{1}{e^{k't}} \quad (4)$$

Figure 8a depicts the fitting curves of $\ln(M_0/M)$ versus the depolymerization time t. A linear relationship between $\ln(M_0/M)$ and t is observed for all of the medium/long-chain terephthalic polyesters, indicating that the applied kinetic model could well describe the depolymerization process. The reaction rate constant k' is also determined from the slopes of the $\ln(M_0/M)$ vs t curves. Since PET and PBT do not undergo depolymerization at a low temperature of 140 °C, their reaction rate constant k' is evaluated to be ~0 under this condition. The k' values of PHT, POT, PDT, and PDeT are determined to be 0.015, 0.019, 0.031, and 0.029 min^{-1} at 140 °C, respectively. It can be concluded that the depolymerization reaction rate of terephthalic polyesters at 140 °C continuously increases as n_{CH_2} increases from 4 to 10. However, for PDeT having the longest chain length ($n_{CH_2} = 12$), the depolymerization reaction rate slightly decreases, which might be due to the low density of ester bonds in polyester.

https://doi.org/10.1021/acs.macromol.4c01793
Macromolecules 2025, 58, 550−561

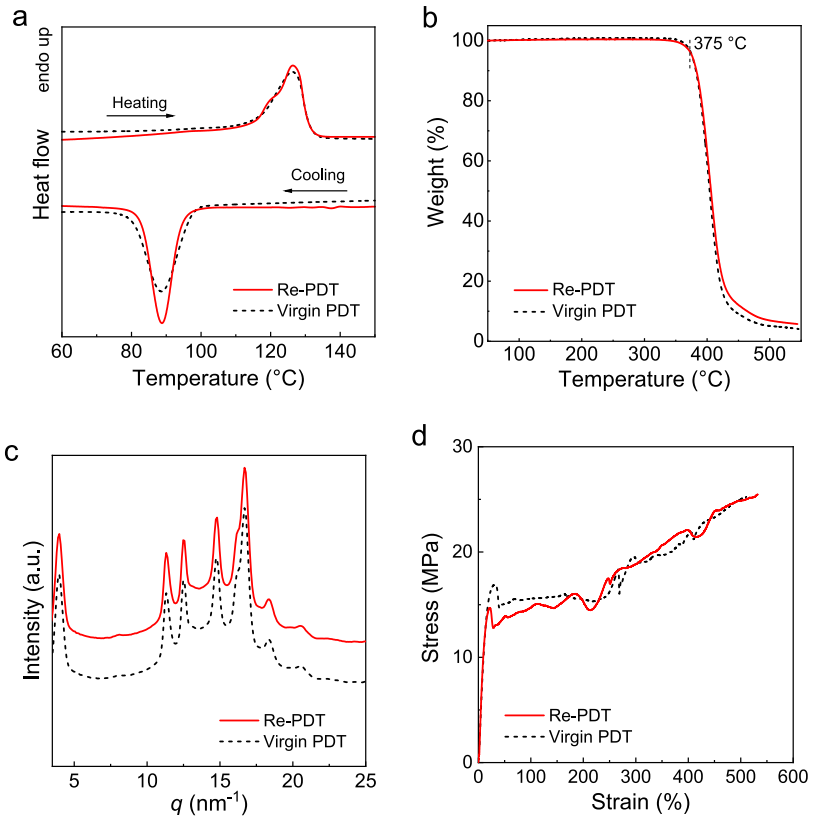

Figure 9. Comparison of the structures and physical properties of recycled and virgin PDT. (a) DSC curves collected upon cooling from melt state and subsequent heating at 10 °C/min; (b) TGA curves; (c) WAXS profiles; (d) strain−stress curves. For the uniaxial stretching and WAXS experiments, all samples were treated by isothermal melt crystallization at T_c = 100 °C for 1 h before measurements.

The theoretical depolymerized ratio (R_d) of terephthalic polyesters at different times was also calculated according to eq 4 and the evolutions of R_d with reaction time t are shown in Figure 8b. The theoretical calculation shows that the medium/long-chain terephthalic polyesters (n_{CH_2} = 6−12) are able to achieve 99% of recovery within 146−310 min, which is among the highest depolymerization efficiency reported for the long-chain polyesters in methanol (at 120−150 °C).[24,55] Such catalyst-free recycling at low energy input and high recovery rate is much more effective than that of PET (usually at 180−250 °C, >3 h with catalyst).[56] These results suggest that medium- and long-chain terephthalic polyesters could be chemically recycled under mild conditions at a fast reaction rate, making them a good type of sustainable plastic.

Physical Properties of Chemically Recycled Terephthalic Polyesters. To achieve the closed-loop chemical recycling of terephthalic polyesters, the recycled monomers obtained from depolymerization were repolymerized into the polyesters. Still taking PDT as an example, recovered DMT and 1,10-DDO (Figure 7) were used to synthesize PDT again by melt polycondensation. The repolymerized polyester was denoted as Re-PDT and the initial polyester before depolymerization was denoted as virgin PDT. The intrinsic viscosity of Re-PDT is determined to be 1.08 dL/g, which is very similar to that of virgin PDT (1.07 dL/g, Table 1), indicating the similar molecular weights between the initial polyester and the recycled one.

In addition to the molecular characteristics, the thermal and mechanical properties of recycled PDT were also characterized and compared with those of virgin PDT. Figure 9a−d shows the DSC, TGA, WAXS, and stress−strain curves of recycled and virgin PDTs. As depicted in Figure 9a, both the recycled and virgin PDTs exhibit a single crystallization and melting peak in the heating and cooling scans, with similar T_c (~89.0, 88.8 °C), T_m (126.5, 126.3 °C), ΔH_c (−56.2, −55.3 J/g), and ΔH_m (49.2, 49.6 J/g) values. The TGA results depicted in Figure 9b show that both the recycled and virgin PDT have a 5% degradation temperature of 375 °C, indicating that there is no significant difference in the thermal stability of the two samples. The crystal structure of recycled PDT after isothermal crystallization at 100 °C is also characterized. According to the WAXS curves shown in Figure 9c, similar characteristic diffraction peaks at q = 4.0, 11.3, 12.5, 14.7, and 16.7 nm^{-1} are detected for both PDTs, indicating that the crystalline structure of recycled polyester is completely consistent with that of the initial sample before depolymerization. Finally, the mechanical properties of recycled and virgin PDTs were measured. As can be seen from Figure 9d, the yield strength, Young's modulus, and strain at break of recycled PDT are around 14.6, 150 MPa, and 530%, respectively (red curve), which are all comparable to the mechanical properties of virgin PDT (dashed black curve). These results imply that the terephthalic polyester recovered through the proposed closed-loop chemical recycling route still retains good physical properties compared with virgin materials.

CONCLUSIONS

In this study, a series of medium/long-chain terephthalic polyesters with different methylene sequence lengths (n_{CH_2} = 6, 8, 10, 12) and high molecular weights were successfully

https://doi.org/10.1021/acs.macromol.4c01793
Macromolecules 2025, 58, 550−561

synthesized, and their thermal properties, crystalline structure, mechanical properties, and chemical recycling performance were investigated. All polyesters show good crystallizability; their T_m decreases and ΔH_m increases gradually as n_{CH_2} increases from 2 to 12. All polyesters adopt a triclinic crystal lattice, while their lamellar structures are slightly different. The d_{ac}, d_a, and d_c of terephthalic polyesters increase with a greater n_{CH_2}. Compared with short-chain terephthalic polyesters such as PET and PBT, medium/long-chain terephthalic polyesters exhibit improved ductility due to enhanced chain mobility. Owing to the relatively lower T_m, fast crystallization rate, and superior flexibility, the medium- and long-chain terephthalic polyesters have good melt processing ability and dyeability, as manifested by their excellent 3D printing behavior. In addition, the medium/long-chain terephthalic polyesters are chemically recyclable and can depolymerize into monomers under mild conditions (~140 °C). The monomers obtained by depolymerization can be reused to synthesize again the according polyesters. This study provides new ideas for the closed-loop chemical recycling and practical application of medium/long-chain terephthalic polyesters, which helps to promote the development of green recyclable polymers with advanced performances.

■ ASSOCIATED CONTENT

Supporting Information

The Supporting Information is available free of charge at https://pubs.acs.org/doi/10.1021/acs.macromol.4c01793.

Experimental section; determination of T_g; determination of crystalline and amorphous layer thickness; determination of crystallinity; ^{1}H NMR spectra of recycled diols (PDF)

■ AUTHOR INFORMATION

Corresponding Authors

Shanshan Xu − *State Key Laboratory of Chemical Engineering, College of Chemical and Biological Engineering, Zhejiang University, Hangzhou 310058, China; School of Materials Science and Engineering, The Key Laboratory of Material Processing and Mold of Ministry of Education, Henan Key Laboratory of Advanced Nylon Materials and Application, Zhengzhou University, Zhengzhou 450000, China*; Email: ssxu@zzu.edu.cn

Pengju Pan − *State Key Laboratory of Chemical Engineering, College of Chemical and Biological Engineering, Zhejiang University, Hangzhou 310058, China; Institute of Zhejiang University-Quzhou, Quzhou 324000, China*; orcid.org/0000-0001-6924-5485; Email: panpengju@zju.edu.cn

Authors

Junfeng Liu − *State Key Laboratory of Chemical Engineering, College of Chemical and Biological Engineering, Zhejiang University, Hangzhou 310058, China; Institute of Zhejiang University-Quzhou, Quzhou 324000, China*

Jianfei Xia − *State Key Laboratory of Chemical Engineering, College of Chemical and Biological Engineering, Zhejiang University, Hangzhou 310058, China*

Chang Zeng − *State Key Laboratory of Chemical Engineering, College of Chemical and Biological Engineering, Zhejiang University, Hangzhou 310058, China*

Chengtao Yu − *State Key Laboratory of Chemical Engineering, College of Chemical and Biological Engineering, Zhejiang University, Hangzhou 310058, China; Institute of Zhejiang University-Quzhou, Quzhou 324000, China*; orcid.org/0000-0002-3656-0582

Ying Zheng − *State Key Laboratory of Chemical Engineering, College of Chemical and Biological Engineering, Zhejiang University, Hangzhou 310058, China; Institute of Zhejiang University-Quzhou, Quzhou 324000, China*; orcid.org/0000-0002-2379-6342

Bao Wang − *State Key Laboratory of Chemical Engineering, College of Chemical and Biological Engineering, Zhejiang University, Hangzhou 310058, China; Institute of Zhejiang University-Quzhou, Quzhou 324000, China*

Complete contact information is available at: https://pubs.acs.org/10.1021/acs.macromol.4c01793

Notes

The authors declare no competing financial interest.

■ ACKNOWLEDGMENTS

This research was financially supported by the National Natural Science Foundation of China (U22A20400), the National Natural Science Foundation of Zhejiang Province (LHDMZ23E030001), and the Key R&D Research Program of Zhejiang Province (2023C01104).

■ REFERENCES

(1) Geyer, R.; Jambeck, J. R.; Law, K. L. Production, Use, and Fate of All Plastics Ever Made. *Sci. Adv.* **2017**, *3*, 19−24.

(2) Lambert, S.; Wagner, M. Environmental Performance of Bio-Based and Biodegradable Plastics: The Road Ahead. *Chem. Soc. Rev.* **2017**, *46*, 6855−6871.

(3) Haider, T. P.; Völker, C.; Kramm, J.; Landfester, K.; Wurm, F. R. Plastics of the Future? The Impact of Biodegradable Polymers on the Environment and on Society. *Angew. Chem., Int. Ed.* **2019**, *58*, 50−62.

(4) Zhang, Q.; Song, M.; Xu, Y.; Wang, W.; Wang, Z.; Zhang, L. Bio-Based Polyesters: Recent Progress and Future Prospects. *Prog. Polym. Sci.* **2021**, *120*, No. 101430.

(5) Larrañaga, A.; Lizundia, E. A Review on the Thermomechanical Properties and Biodegradation Behaviour of Polyesters. *Eur. Polym. J.* **2019**, *121*, No. 109296.

(6) Rabnawaz, M.; Wyman, I.; Auras, R.; Cheng, S. A Roadmap towards Green Packaging: The Current Status and Future Outlook for Polyesters in the Packaging Industry. *Green Chem.* **2017**, *19*, 4737−4753.

(7) Yamamoto, Y.; Hoshina, H.; Sato, H. Differences in Intermolecular Interactions and Flexibility between Poly(ethylene terephthalate) and Poly(Butylene Terephthalate) Studied by Far-Infrared/Terahertz and Low-Frequency Raman Spectroscopy. *Macromolecules* **2021**, *54*, 1052−1062.

(8) Tasaki, M.; Yamamoto, H.; Yoshioka, T.; Hanesaka, M.; Ninh, T. H.; Tashiro, K.; Jeon, H. J.; Choi, K. B.; Jeong, H. S.; Song, H. H.; Ree, M. H. Microscopically-Viewed Relationship between the Chain Conformation and Ultimate Young's Modulus of a Series of Arylate Polyesters with Long Methylene Segments. *Polymer* **2014**, *55*, 1799−1808.

(9) Shi, C.; Quinn, E. C.; Diment, W. T.; Chen, E. Y.-X. Recyclable and (Bio)Degradable Polyesters in a Circular Plastics Economy. *Chem. Rev.* **2024**, *124*, 4393−4478.

(10) Brisse, F.; Palmer, A.; Moss, B.; Dorset, D.; Roughead, W. A.; Miller, D. P. Poly(hexamethylene terephthalate)-II. The Crystal Structure of Forms I and II, from Electron and X-Ray Diffraction, and Packing Analyses. *Eur. Polym. J.* **1984**, *20*, 791−797.

(11) Sun, Y. S. Temperature-Resolved SAXS Studies of Morphological Changes in Melt-Crystallized Poly(hexamethylene terephthalate) and Its Melting upon Heating. *Polymer* **2006**, *47*, 8032−8043.

(12) Yen, K. C.; Woo, E. M. Thermal, Spectroscopy, and Morphological Studies on Polymorphic Crystals in Poly(heptamethylene terephthalate). *Polymer* **2009**, *50*, 662−669.
(13) Flores, I.; Martínez De Ilarduya, A.; Sardon, H.; Müller, A. J.; Muñoz-Guerra, S. Synthesis of Aromatic-Aliphatic Polyesters by Enzymatic Ring Opening Polymerization of Cyclic Oligoesters and Their Cyclodepolymerization for a Circular Economy. *ACS Appl. Polym. Mater.* **2019**, *1*, 321−325.
(14) Guo, Z.; Warlin, N.; Mankar, S. V.; Sidqi, M.; Andersson, M.; Zhang, B.; Nilsson, E. Development of Circularly Recyclable Low Melting Temperature Bicomponent Fibers toward a Sustainable Nonwoven Application. *ACS Sustainable Chem. Eng.* **2021**, *9*, 16778−16785.
(15) Kunduru, K. R.; Basu, A.; Haim Zada, M.; Domb, A. J. Castor Oil-Based Biodegradable Polyesters. *Biomacromolecules* **2015**, *16*, 2572−2587.
(16) Hillmyer, M. A. The Promise of Plastics from Plants. *Science* **2017**, *358*, 868−870.
(17) Ortmann, P.; Mecking, S. Long-Spaced Aliphatic Polyesters. *Macromolecules* **2013**, *46*, 7213−7218.
(18) Zhao, J. Z.; Yue, T. J.; Ren, B. H.; Lu, X. B.; Ren, W. M. Closed-Loop Recycling of Sulfur-Rich Polymers with Tunable Properties Spanning Thermoplastics, Elastomers, and Vitrimers. *Nat. Commun.* **2024**, *15*, No. 3002.
(19) Haider, T.; Shyshov, O.; Suraeva, O.; Lieberwirth, I.; Von Delius, M.; Wurm, F. R. Long-Chain Polyorthoesters as Degradable Polyethylene Mimics. *Macromolecules* **2019**, *52*, 2411−2420.
(20) Zhou, L.; Qin, P.; Wu, L.; Li, B. G.; Dubois, P. Potentially Biodegradable "Short-Long" Type Diol-Diacid Polyesters with Superior Crystallizability, Tensile Modulus, and Water Vapor Barrier. *ACS Sustainable Chem. Eng.* **2021**, *9*, 17362−17370.
(21) Xu, Z. W.; Pan, J. L.; Xu, J.; Cheng, W. M.; Li, Z. L.; Cheng, C. Recyclable, Reprocessable, Anticorrosive, and Hydrolysis-Resistant Long-Chain Aliphatic Polycarbonates as Polyethylene-like Materials. *ACS Appl. Polym. Mater.* **2024**, *6*, 1551−1562.
(22) Eck, M.; Mecking, S. Closed-Loop Recyclable and Non-persistent Polyethylene-like Polyesters. *Acc. Chem. Res.* **2024**, *57*, 971−980.
(23) Ortmann, P.; Wimmer, F. P.; Mecking, S. Long-Spaced Polyketones from ADMET Copolymerizations as Ideal Models for Ethylene/CO Copolymers. *ACS Macro Lett.* **2015**, *4*, 704−707.
(24) Häußler, M.; Eck, M.; Rothauer, D.; Mecking, S. Closed-Loop Recycling of Polyethylene-like Materials. *Nature* **2021**, *590*, 423−427.
(25) Menges, M. G.; Penelle, J.; Le Fevere De Ten Hove, C.; Jonas, A. M.; Schmidt-Rohr, K. Characterization of Long-Chain Aliphatic Polyesters: Crystalline and Supramolecular Structure of PE22,4 Elucidated by X-Ray Scattering and Nuclear Magnetic Resonance. *Macromolecules* **2007**, *40*, 8714−8725.
(26) Pepels, M. P. F.; Hansen, M. R.; Goossens, H.; Duchateau, R. From Polyethylene to Polyester: Influence of Ester Groups on the Physical Properties. *Macromolecules* **2013**, *46*, 7668−7677.
(27) Stempfle, F.; Ortmann, P.; Mecking, S. Long-Chain Aliphatic Polymers to Bridge the Gap between Semicrystalline Polyolefins and Traditional Polycondensates. *Chem. Rev.* **2016**, *116*, 4597−4641.
(28) Ji, L.; Meng, J.; Li, C.; Wang, M.; Jiang, X. From Polyester Plastics to Diverse Monomers via Low-Energy Upcycling. *Adv. Sci.* **2024**, *11*, No. 2403002.
(29) Billiet, S.; Trenor, S. R. 100th Anniversary of Macromolecular Science Viewpoint: Needs for Plastics Packaging Circularity. *ACS Macro Lett.* **2020**, *9*, 1376−1390.
(30) Rochman, C. M.; Browne, M. A.; Halpern, B. S.; Hentschel, B. T.; Hoh, E.; Karapanagioti, H. K.; Rios-Mendoza, L. M.; Takada, H.; Teh, S.; Thompson, R. C. Policy: Classify Plastic Waste as Hazardous. *Nature* **2013**, *494*, 169−170.
(31) El Darai, T.; Ter-Halle, A.; Blanzat, M.; Despras, G.; Sartor, V.; Bordeau, G.; Lattes, A.; Franceschi, S.; Cassel, S.; Chouini-Lalanne, N.; Perez, E.; Déjugnat, C.; Garrigues, J. C. Chemical Recycling of Polyester Textile Wastes: Shifting towards Sustainability. *Green Chem.* **2024**, *26*, 6857−6885.
(32) Ghosal, K.; Nayak, C. Recent Advances in Chemical Recycling of Polyethylene Terephthalate Waste into Value Added Products for Sustainable Coating Solutions-Hope *vs.* Hype. *Mater. Adv.* **2022**, *3*, 1974−1992.
(33) Weng, Y.; Hong, C.; Bin; Zhang, Y.; Liu, H. Catalytic Depolymerization of Polyester Plastics toward Closed-Loop Recycling and Upcycling. *Green Chem.* **2024**, *26*, 571−592.
(34) MacLeod, M.; Arp, H. P. H.; Tekman, M. B.; Jahnke, A. The Global Threat from Plastic Pollution. *Science* **2021**, *373*, 61−65.
(35) Hong, M.; Chen, E. Y. X. Completely Recyclable Biopolymers with Linear and Cyclic Topologies *via* Ring-Opening Polymerization of γ-Butyrolactone. *Nat. Chem.* **2016**, *8*, 42−49.
(36) Eck, M.; Schwab, S. T.; Nelson, T. F.; Wurst, K.; Iberl, S.; Schleheck, D.; Link, C.; Battagliarin, G.; Mecking, S. Biodegradable High-Density Polyethylene-like Material. *Angew. Chem.* **2023**, *135*, 1−4.
(37) Sathe, D.; Zhou, J.; Chen, H.; Su, H. W.; Xie, W.; Hsu, T. G.; Schrage, B. R.; Smith, T.; Ziegler, C. J.; Wang, J. Olefin Metathesis-Based Chemically Recyclable Polymers Enabled by Fused-Ring Monomers. *Nat. Chem.* **2021**, *13*, 743−750.
(38) Ortmann, P.; Heckler, I.; Mecking, S. Physical Properties and Hydrolytic Degradability of Polyethylene-like Polyacetals and Polycarbonates. *Green Chem.* **2014**, *16*, 1816−1827.
(39) Pepels, M. P. F.; Koeken, R. A. C.; Van Der Linden, S. J. J.; Heise, A.; Duchateau, R. Mimicking (Linear) Low-Density Polyethylenes Using Modified Polymacrolactones. *Macromolecules* **2015**, *48*, 4779−4792.
(40) Haider, T. P.; Suraeva, O.; Lieberwirth, I.; Paneth, P.; Wurm, F. R. RNA-Inspired Intramolecular Transesterification Accelerates the Hydrolysis of Polyethylene-like Polyphosphoesters. *Chem. Sci.* **2021**, *12*, 16054−16064.
(41) Cangialosi, D. Dynamics and Thermodynamics of Polymer Glasses. *J. Phys.: Condens. Matter* **2014**, *26*, No. 153101.
(42) Jiang, Y.; Woortman, A. J. J.; Alberda Van Ekenstein, G. O. R.; Loos, K. A Biocatalytic Approach towards Sustainable Furanic-Aliphatic Polyesters. *Polym. Chem.* **2015**, *6*, 5198−5211.
(43) Ran, S.; Wang, Z.; Burger, C.; Chu, B.; Hsiao, B. S. Mesophase as the Precursor for Strain-Induced Crystallization in Amorphous Poly(ethylene terephthalate) Film. *Macromolecules* **2002**, *35*, 10102−10107.
(44) Hall, I. H.; Pass, M. G. Chain Conformation of Poly(tetramethylene terephthalate) and Its Change with Strain. *Polymer* **1976**, *17*, 807−816.
(45) Sago, T.; Itagaki, H.; Asano, T. Onset of Forming Ordering in Uniaxially Stretched Poly(Ethylene Terephthalate) Films Due to π-π Interaction Clarified by the Fluorescence Technique. *Macromolecules* **2014**, *47*, 217−226.
(46) Xia, J.; Ni, L.; Zeng, C.; Wang, B.; Zhang, R.; Sun, C.; Song, J.; Liu, J.; Yu, C.; Zheng, Y.; Pan, P. Temperature-Dependent Triple Crystal Polymorphism of Poly(Hexamethylene Terephthalate): Long-Range Ordered Mesophase Formation and Crystal Structure-Property Relationships. *Macromolecules* **2024**, *57*, 7369−7380.
(47) Flores, I.; Pérez-Camargo, R. A.; Gabirondo, E.; Caputo, M. R.; Liu, G.; Wang, D.; Sardon, H.; Müller, A. J. Unexpected Structural Properties in the Saturation Region of the Odd-Even Effects in Aliphatic Polyethers: Influence of Crystallization Conditions. *Macromolecules* **2022**, *55*, 584−594.
(48) Wu, X.; Liu, C.; Zhu, Z.; Ngai, K. L.; Wang, L. M. Nature of the Sub-Rouse Modes in the Glass-Rubber Transition Zone of Amorphous Polymers. *Macromolecules* **2011**, *44*, 3605−3610.
(49) Men, Y. Critical Strains Determine the Tensile Deformation Mechanism in Semicrystalline Polymers. *Macromolecules* **2020**, *53*, 9155−9157.
(50) Zeng, Y.; Xu, Y. T.; Zhang, J.; Xu, L.; Ji, X.; Lin, H.; Zhong, G. J.; Li, Z. M. Coupling Effect of Mechanical and Thermal Rejuvenation for Polystyrene: Toward High Performance of Stiffness, Ductility, and Transparency. *Macromolecules* **2021**, *54*, 8875−8885.
(51) Shelby, M. D.; Hill, A. J.; Burgar, M. I.; Wilkes, G. L. Effects of Molecular Orientation on the Physical Aging and Mobility of

https://doi.org/10.1021/acs.macromol.4c01793
Macromolecules 2025, 58, 550−561

Polycarbonate-Solid State NMR and Dynamic Mechanical Analysis. *J. Polym. Sci., Part B: Polym. Phys.* **2001**, *39*, 32−46.
(52) Xu, S.; Zhou, J.; Pan, P. Strain-Induced Multiscale Structural Evolutions of Crystallized Polymers: From Fundamental Studies to Recent Progresses. *Prog. Polym. Sci.* **2023**, *140*, No. 101676.
(53) Capello, C.; Fischer, U.; Hungerbühler, K. What Is a Green Solvent? A Comprehensive Framework for the Environmental Assessment of Solvents. *Green Chem.* **2007**, *9*, 927−993.
(54) Wan, B. Z.; Kao, C. Y.; Cheng, W. H. Kinetics of Depolymerization of Poly(ethylene terephthalate) in a Potassium Hydroxide Solution. *Ind. Eng. Chem. Res.* **2001**, *40*, 509−514.
(55) Schwab, S. T.; Baur, M.; Nelson, T. F.; Mecking, S. Synthesis and Deconstruction of Polyethylene-Type Materials. *Chem. Rev.* **2024**, *124*, 2327−2351.
(56) Clark, R. A.; Shaver, M. P. Depolymerization within a Circular Plastics System. *Chem. Rev.* **2024**, *124*, 2617−2650.

https://doi.org/10.1021/acs.macromol.4c01793
Macromolecules 2025, 58, 550−561